Full Length Article

Durability of AZ31 magnesium biodegradable alloys polydopamine aided. Part 2: Ageing in Hank's solution

Anna Carangelo*, Annalisa Acquesta, Tullio Monetta

Department of Chemical Engineering, Materials and Industrial Production, University of Napoli Federico II, Piazzale Tecchio 80, 80125 Napoli, Italy

Abstract

Magnesium alloys are candidates as biodegradable medical materials due to their biocompatibility and favorable mechanical properties. Unfortunately, the high corrosion rate in physiological media and the release of hydrogen, limit their widespread use in biomedical applications. In this work, an intermediate coating based on polydopamine (PDOPA), between Mg substrate and an organic coating, was used to decreasing the degradation rate of AZ31 magnesium alloy, during the long-term exposure in simulated body fluid. Electrochemical Impedance Spectroscopy measurements were carried out to study the corrosion resistance of samples. Results demonstrated that the PDOPA interlayer determined the reduction of the substrate degradation rate. The results were interpreted supposing a synergistic effect which occurred when PDOPA and the organic coating were used together.

1. Introduction

Metallic materials, such as stainless steel and titanium alloys, are widely used to produce medical devices, such as implants, prosthesis and so on. The main trait required for those materials is that they have not degraded in the human body, realizing armful species. Then, if the medical device has to perform its function for a limited amount of time, it is necessary a second surgical procedure after tissues have healed to remove it. On this matter, magnesium alloys have been considered to be a potential material for temporary biodegradable devices with promising results [1,2]. The advantages of Mg are high biocompatibility and favorable mechanical properties. Conversely, the main limitations of the medical use of magnesium alloys are their fast corrosion rate when in contact with body fluids. Moreover, the release of hydrogen evolution and alkalization of the site have to be taken into account. On the other hand, it is noteworthy that medical devices need

surface treatments for improving their corrosion resistance, antibacterial activity and cellular adhesions [3–5]. In order to improve the surface properties of devices, an organic coating can be used. Some biodegradable polymers have been tested and used, like, polycaprolactone (PCL) and polylactic acid (PLA) [6–8]. They were considered for their slow degradation rate, but it has been shown that their degradation accelerated due to the pH variation in the surrounding of degradation site [9]. Chen et al. [9], i.e., showed that homogeneous PCL and PLA coatings were successfully prepared on the surface of high purity magnesium but the alkaline environment degraded the coatings, increasing the corrosion rate of the metallic substrate.

A procedure to overcome the problem could be the usage of a biocompatible and biodegradable intermediate coating interposed between the metal substrate and the external coating, in order to slow down the metal dissolution rate while increasing the coating adhesion. A nature-inspired solution could be found based on the adhesion mechanism used by mussels to stick to various solid surfaces [10,11] in a wet and dry environment [12]. The remarkable feature of adhe-

---

Table 1
Adopted nomenclature used to identify the samples.

Abbreviations of investigated samples	Acronym description of the sample
LM10	Mechanical lapped and chemical etched
LMP	As LM10 and PDOPA coated
LME	As LM10 and epoxy resin coated
LMPE	As LM10 coated by PDOPA and epoxy resin

sion of the mussel is due to fibres containing polydopamine. PDOPA can be synthesized in the laboratory and, it has been demonstrated, to be biocompatible, biodegradable, to promote cell adhesion and have no cytotoxic effects [13–15]. Nevertheless, few papers [16–19] deal with the use of PDOPA as an insulating layer to slow down the corrosion rate.

This study examines the corrosion behavior of AZ31 magnesium samples when coated using an organic resin and the PDOPA intermediate layer, even after a long time of immersion to Hank's solution.

2. Experimental

The nominal composition of the AZ31 magnesium alloy samples used in this work was: %Al (2.5–3.5), %Zn (0.7–1.3), %Mn (0.2–1), %Si(0.05), %Cu (0.01), %Fe (>0.05), % Ni(>0.05), %Others (0.4), and %Mg (balance); and was supplied by Goodfellow U.K., Llangollen, UK.

The dimensions of the sample used in the experiments were 130 mm × 70 mm × 3 mm. The specimens were ground with SiC paper from P240 to P1200, to obtain the appropriate surface topography [20,21], using pure ethanol as lubricant, as suggested by Geels et al. [22], in order to remove contamination layers and native oxide. The samples were pre-treated in hydrochloride acid (HCl) solution, bought from Sigma-Aldrich (Sigma-Aldrich, Milano, Italy). In particular, the specimens were immersed in the solution for 10 s and stirred at 300 rpm. Then, the specimens were rinsed in the deionized water and dried in air.

After the pre-treatment, the specimens were coated with polydopamine (PDOPA) film. The polymerization process of PDOPA was carried out by immersion of the samples in the aqueous solution containing 2 mg/ml of dopamine hydrochloride and 10 mM of trizma base (purchased from Sigma-Aldrich, Milano, Italy) [23,24]. The specimens were immersed in the solution for 24 h and stirred at 500 rpm at pH of 8.5. The pH values were recorded using pH meter (Hanna Instruments, Romania). At the last, the samples were rinsed by using deionized water and then cured for 10 min at 150 °C. Some samples were, then, coated with water-based epoxy resin (Sikkens Wapex 660, Torino, Italy) by using doctor blade technique (Gardco, Florida, USA) and were cured in an oven for 10 min at 150 °C. The details of the choice of that type of resin have been discussed elsewhere [20].

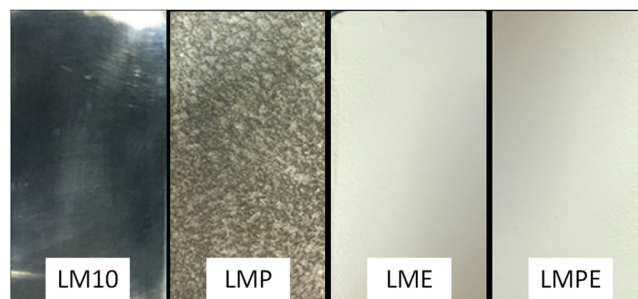The adopted nomenclature used in order to identify the samples is reported in Table 1.

Fig. 1. Images of (a) LM10 sample, (b) sample PDOPA coated (LMP), (c) sample covered by an organic coating (LME) and (d) sample covered by PDOPA and organic coating (LMPE) [20].

The electrochemical properties of samples have been investigated by the Electrochemical Impedance Spectroscopy (EIS) (Gamry Interface 1000, Gamry Instruments, Pennsylvania, USA) in Hank's solution [25,26]. The solution was bought from Carlo Erba Reagents, Milano, Italy and the EIS was carried out at 37 °C ± 0.5 °C till 21 days. A three-electrode cell was used, with the specimen as working electrode, a saturated calomel as a reference electrode and a platinum cathode. The exposed samples area was 2.83 cm². The impedance spectra were acquired applying a sinusoidal perturbation with an amplitude of 10 mV over the frequency range from 100 kHz to 2 mHz. Before EIS measurements, the open circuit potential (OCP) was monitored for 90 min. Each electrochemical test was repeated three times in order to evaluate the reproducibility and the curves were almost overlapping. Whereas the electrochemical polarization measurements were performed as reported in a previous work [20] and herein not reported.

The morphologies of all samples were observed, before and after electrochemical tests, by Scanning Electron Microscope (SEM) (Hitachi TM3000, Hitachi, Japan). Furthermore, to gain insight into the thickness of the PDOPA and epoxy resin applied on the samples, the cross-sections surfaces were observed too. The chemical compositions were determined by Energy Dispersive Spectroscopy (EDS) system (Oxford Instruments Swift ED3000).

3. Results and discussion

The pictures of the specimens after different treatments are shown in Fig. 1. The aspect of the LM10 sample was due to the chemical pre-treatment so that the surface appeared shiny; the LMP sample revealed a variation in color (dark and pale grey) due to the change in coating thickness, as well discussed in detail elsewhere and not reported here for brevity [20]; the LME and the LMPE samples exhibited the same appearance due to the external epoxy resin color.

Before observing the surfaces by using SEM, the samples were incorporated into a conductive resin for hot embedding. The cross-sections images of the (i) PDOPA layer, (ii) epoxy resin coating and (iii) combination of PDOPA and organic resin are reported in Figs. 2, 3 and 4, respectively. It is noteworthy that the thickness of PDOPA layer was, in the average,
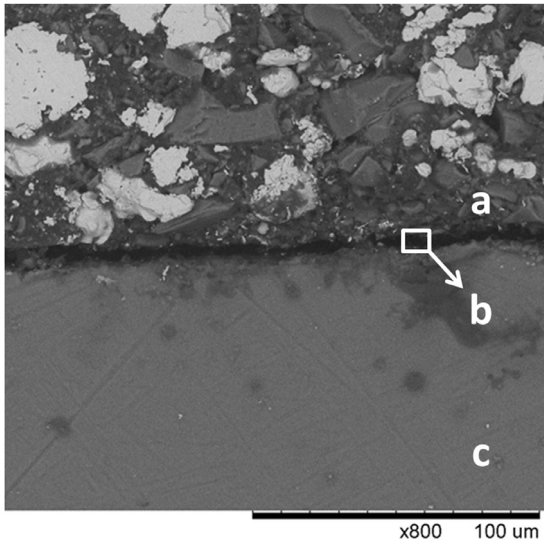
Fig. 2. Scanning electron microscopy images of the LMP cross-section sample: (a) conductive resin used for hot embedding, (b) PDOPA layer and (c) magnesium substrate.
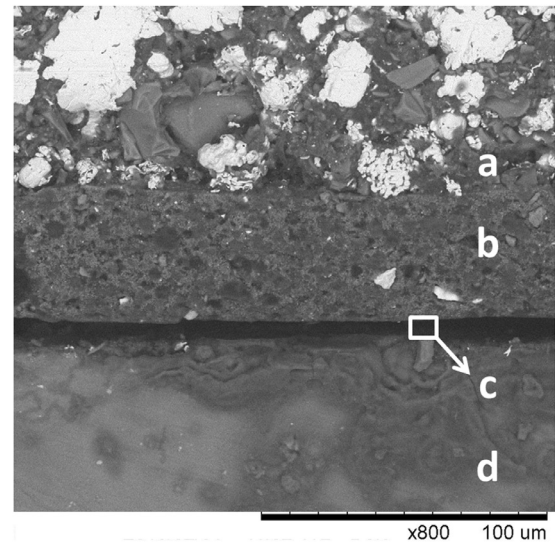

Fig. 4. Scanning electron microscopy images of the LMPE cross-section sample: (a) conductive resin used for hot embedding, (b) epoxy resin layer, (c) PDOPA layer and (d) magnesium substrate.
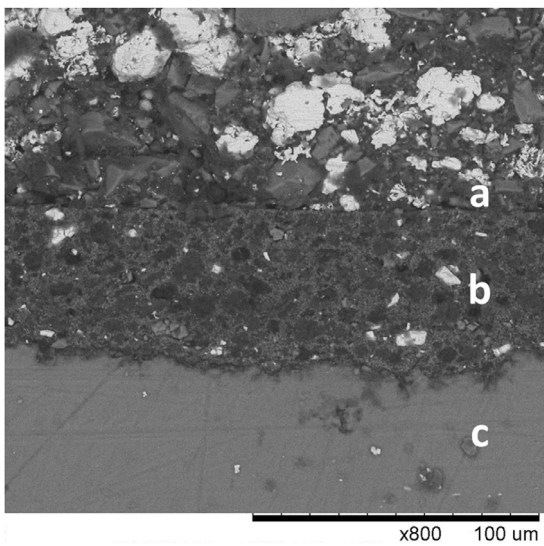

Fig. 3. Scanning electron microscopy images of the LME cross-section sample: (a) conductive resin used for hot embedding, (b) epoxy resin layer and (c) magnesium substrate.

Fig. 5. Impedance modulus (a) and phase angle (b) of LM10 sample acquired at 37 °C in Hank's solution.

estimated in 5 μm (see Fig. 2) while the width of the epoxy resin coating was measured in 48 μm circa (see Fig. 3).

The EIS spectra obtained studying the bare LM10 sample at the beginning of the test campaign (0 days of immersion in the test solution) and after 2, 7, 10 and 21 days of immersion, are reported in Fig. 5, in which the impedance modulus and phase angle plots are represented as a function of the immersion time of the sample in the test solution.

The impedance modulus evaluated at low frequencies, at the beginning of the test, reached a value of $5.5 \cdot 10^3 \Omega$ cm³. That value increased until $3.2 \cdot 10^4 \Omega$ cm² , after two days, due to the formation of the oxide layer on the metallic surface. In fact, it acted as a barrier against corrosion, slowing down
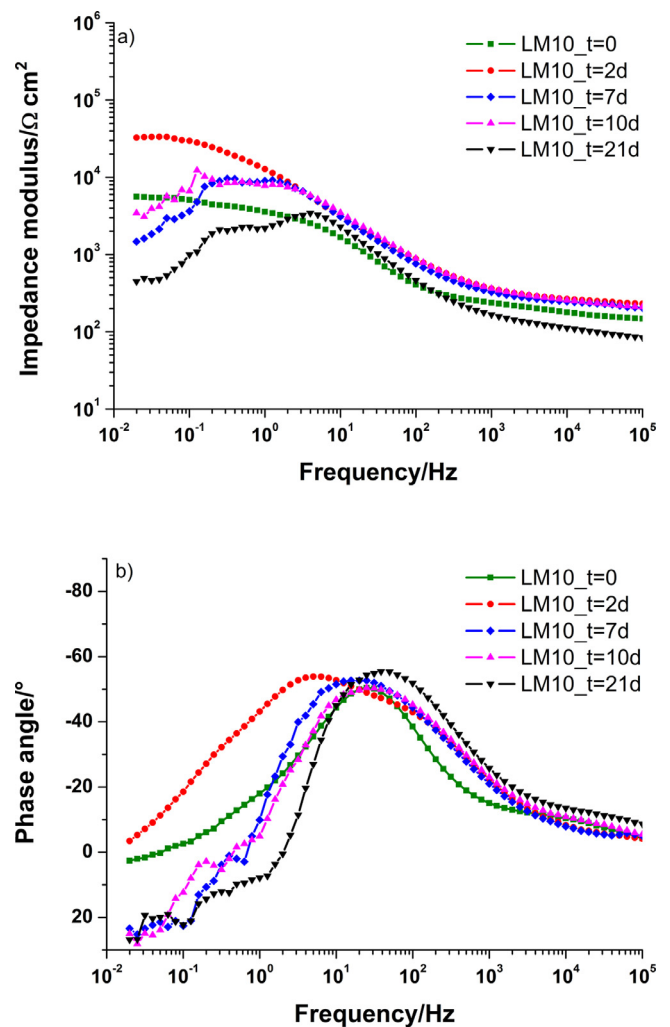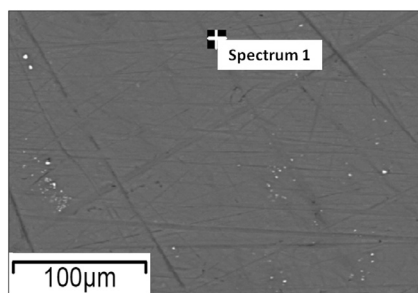
Fig. 6. Scanning electron micrograph of the surface of LM10 sample before immersion in Hank's solution.

Table 2
Surface chemical composition of LM10 sample before exposure in Hank's solution.

Element	Weight%	Weight% σ	Atomic%
Magnesium	96.22	0.16	97.19
Aluminium	2.58	0.09	2.35
Iron	0.15	0.09	0.07
Zinc	1.05	0.10	0.40

the rate of the material degradation process. Even if, the oxide layer could be considered as a passivating film; it, being porous, allowed the direct contact between the metal surface and the aggressive solution. For this reason, the modulus of impedance at low frequencies, after 7 days of immersion in the test solution, decreased. At this stage, the precipitation/solubilisation of salts on the sample surface determined the noisy signal in the EIS spectra and the fluctuation of impedance modulus in subsequent tests. After 10 days the oxide/salts layer grew up and degraded again to 21 days. The peculiarity of the electrochemical behavir of the LM10 sample was the continuous formation and degradation of the oxide/salts layer, which caused, as said, the fluctuation of the impedance modulus at low frequencies, varying in the range between $3.2 \cdot 10^4 \Omega$ cm^2 and $4.5 \cdot 10^2 \Omega$ cm^2. In the same manner, the noisy signal, recorded in the range at low frequencies (10^{-2}–10^0 Hz), could be addressed to the following reasons: (i) the low amplitude of the potential applied and (ii) the rapid evolution of corrosion process during the test and (iii) the formation/dissolution of the thin salts/oxide layer. In addition, experimental data, recorded at 2, 7 and 10 days, highlighted an upward shift of impedance modulus at medium frequencies (i.e. 10^0–10^2 Hz) if compared to the curves obtained at the beginning of the immersion time, demonstrating a decrease of the sample capacitance, due to the presence of porous formed layer at the interface between the metallic substrate and the electrolytic solution. This effect was confirmed by the increase of the phase angle (see Fig. 5b) at the same frequencies.

The picture reported in Fig. 6 shows the SEM micrograph of the LM10 sample as obtained following the mechanical treatments. In the same photo, the area in which the chemical composition of the sample has been evaluated by EDS is highlighted. Data reported in Table 2, clearly showed that the sample has been cleaned in a suitable manner, in fact, surface
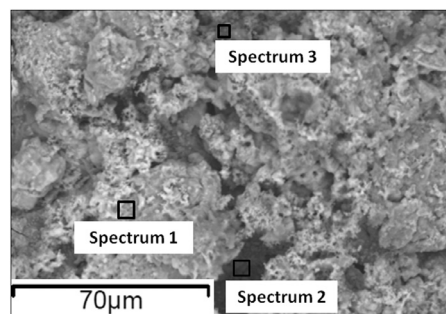

Fig. 7. Scanning electron micrograph of the surface of the LM10 sample after 21 days of immersion in Hank's solution.

Table 3
Surface chemical composition of LM10 sample after 21 days of immersion in Hank's solution.

Element	Weight%			Mean	Standard deviation
	Spectrum 1	Spectrum 2	Spectrum 3		
Carbon	13.43	–	11.39	8.27	7.24
Oxygen	50.81	42.40	22.31	38.51	14.64
Sodium	5.98	7.92	2.93	5.61	2.51
Magnesium	7.76	5.50	1.70	4.99	3.06
Aluminium	0.55	0.53	0.14	0.41	0.23
Phosphorus	6.46	5.27	3.20	4.98	1.65
Chlorine	7.02	19.91	40.92	22.62	17.11
Potassium	0.37	0.75	0.34	0.49	0.23
Calcium	7.62	16.74	17.07	13.81	5.36
Zinc	–	0.98	–	0.33	0.57

composition reflected the chemical composition of the AZ31 alloy, even if a very little quantity of Fe was present due to surface contamination. On the other hand, as the samples were stored in a dry box till the beginning of test campaign, the failure to detect the oxygen on the surface sample was addressed to the EDS sampling depth that is deeper than the thickness of the oxide layer formed on the sample. Moreover, the chemical surface composition was assumed to be constant on the sample surface, in fact, it was not highlighted any substantial changes if the point of analysis was changed.

The picture reported in Fig. 7 showed the SEM micrograph of the LM10 sample after exposure to Hank's solution for 21 days. The spectrum numbers, inside the micrograph, indicated the position in which the spot of the EDS has been addressed to detect the surface chemical composition. The picture clearly showed that the shape of the surface changed significantly if compared to the sample before the immersion in the test solution. The different structure was due to (i) the degradation of the alloy surface when the corrosion phenomena occurring on it; (ii) the formation of an oxide layer and (iii) the deposition of salts consisting of the chemical species supplied by Hank's solution. It is noticeable (see Table 3) that the chemical composition of the surface changed, in a substantial way, when the point of analysis was changed on the surface itself. Table 3 reports the mean value concentration and the standard deviation (SD) of measured values, calculated for each chemical element. Sometimes, the
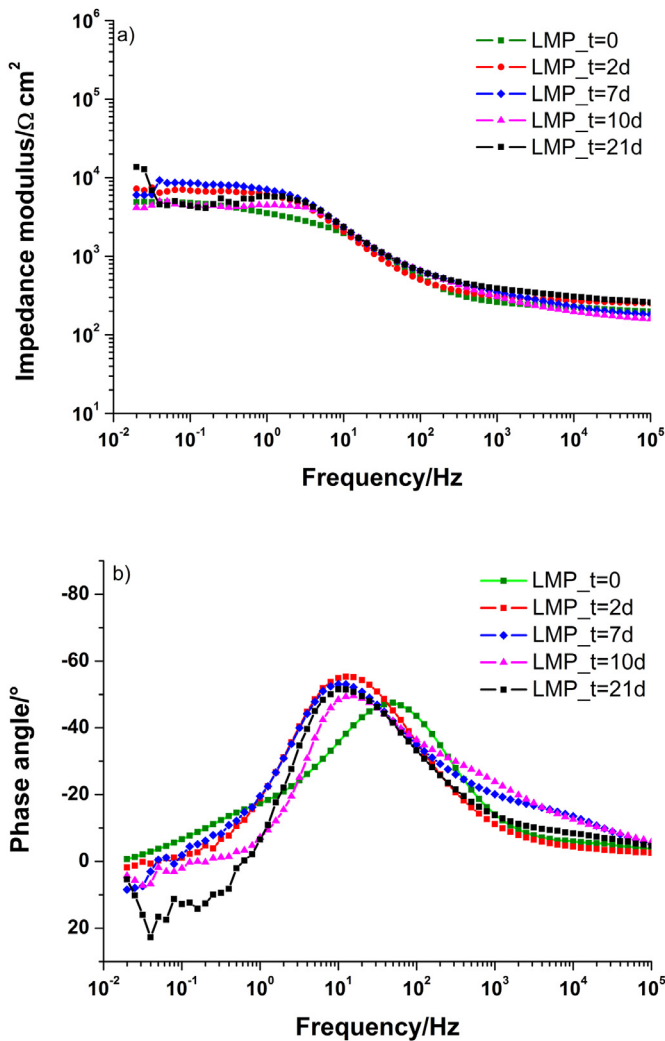
Fig. 8. Impedance modulus (a) and phase angle (b) of LMP sample acquired at 37 °C in Hank's solution.
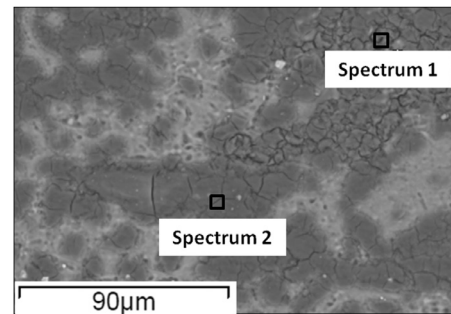

Fig. 9. Scanning electron micrograph of the surface of the LMP sample before immersion in Hank's solution.

Table 4
Surface chemical composition of LMP sample before immersion in Hank's solution.

Element	Weight%	
	Spectrum 1	Spectrum 2
Carbon	23.54	30.41
Nitrogen	5.51	6.74
Oxygen	39.75	39.82
Magnesium	28.83	21.46
Aluminium	1.66	1.58
Zinc	0.71	–

SD assumed a similar value than that measured. Therefore, attention should be paid in reporting the composition experimental values, without acquiring a sufficiently large number of results. In any way, it was clear that the specimen surface was covered by a thin heterogeneous layer of salts and that their precipitation was affected by the Mg^{+2} ions and the pH of the solution [27], as will be discussed better later.

Experimental results, displayed in the Bode plots, obtained testing the LMP sample are reported in Fig. 8.

The shape of impedance modulus and phase angle curves were similar to those of the LM sample, but the variation of the impedance modulus and phase angle occurred in a narrow range of values, indicating a certain amount of stability imposed by the polydopamine coating, even if the layer is not compact caused by cracks formed during the water desorption from the polydopamine layer, during the drying. The impedance modulus, starting from $4.8 \cdot 10^3 \Omega$ cm^2, raised until about $1.4 \cdot 10^4 \Omega$ cm^2 after 21 days of immersion in the test solution. Therefore, it could be stated that the PDOPA layer had a kind of stabilizing effect respect to the

corrosive phenomena occurring at the metal surface, inhibiting the direct contact between the metallic surface and the electrolyte, so that the formation and dissolution of the oxide/salts layer on the sample surface induced smaller variations in the impedance modulus. The stabilizing effect of the PDOPA organic coating was confirmed by looking at the phase angle values (see Fig. 8b). In fact, data showed an increase and a shift toward lower frequencies of the phase angle peak, after the first curve was recorded (at about 50 Hz at $t=0$), but the range frequencies variation was narrow if compared to that exhibited by the LM sample.

Fig. 9 reports the SEM micrograph of the LMP sample before electrochemical tests, where the cracks on the coating surface are clearly visible. The analysis of the EDS results, reported in Table 4, showed that the surface composition, measured in several loci by EDS beam, was quite homogeneous, highlighting the presence of C, O and N due to the PDOPA coating.

The picture reported in Fig. 10 shows the SEM micrograph of the LMP sample after exposure to Hank's solution for 21 days. As was occurred studying the LM sample, the specimen surface was found to be covered by a thin layer constituted by salts precipitated from Hank's solution. While the chemical species composing the layer were, obviously, the same found on the LM sample, the standard deviation of measurements (see Table 5), executed in different places on the surface, was smaller compared to the previous one. So that, the thin PDOPA layer seemed to determine the formation of a more homogeneous film as well as it showed a stabilizing effect on the degradation of the metal substrate as demonstrated by electrochemical tests. It could be concluded that the PDOPA
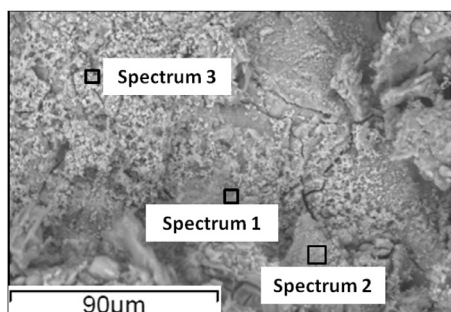
Fig. 10. Scanning electron micrograph of the surface of LMP sample after 21 days of immersion in Hank's solution.

Table 5
Surface chemical composition of LMP sample after 21 days of immersion in Hank's solution.

Element	Weight%			Mean	Standard deviation
	Spectrum 1	Spectrum 2	Spectrum 3		
Carbon	1.64	4.46	4.59	3.56	1.67
Nitrogen	–	–	7.70	2.57	4.44
Oxygen	50.04	47.24	35.94	44.41	7.46
Sodium	0.87	1.17	0.67	0.90	0.25
Magnesium	8.72	8.88	4.60	7.40	2.42
Aluminium	–	0.23	0.24	0.16	0.14
Phosphorus	12.83	14.19	15.00	14.00	1.10
Chlorine	0.90	0.97	–	0.62	0.54
Potassium	0.23	0.29	0.33	0.28	0.05
Calcium	24.78	22.59	30.92	26.10	4.32

Fig. 11. Impedance modulus (a) and phase angle (b) of LME sample acquired at 37 °C in Hank's solution.

layer, did not possess any protective properties as requested by the classical anticorrosive tests (i.e. high impedance modulus), but it performed a protective action on the surface that prevented the metallic substrate rapid deterioration.

Data reported in Fig. 11 represent the impedance modulus and phase angle plots as a function of frequency when the epoxy resin was used to coat the mechanical lapped metal.

As previously stated, the coating used in this work did not contain corrosion inhibitors or any kind of anticorrosive pigments, so that it showed poor corrosion resistance. In addition, in previous papers [28,29], studying the adsorption of water salt solution (3.5 wt% NaCl) in the coating made of the same type of commercial product, was verified that the organic layer was fully saturated by the water in about 2.7 h. Taking into account that the EIS test required time to stabilize the electrical signal and that the duration of the EIS test, as performed it, was of about 90 min, one could affirm that the coating had absorbed about the 80% of the total amount of water it could soak up, during the preparation and execution of the EIS test.

As results, since the beginning of sample immersion in the test solution, the coating exhibited a very low impedance modulus ($1.6 \cdot 10^4 \, \Omega \, cm^4$) which progressively decreased, over the time, to reach the value of $1 \cdot 10^3 \, \Omega \, cm^3$ (see Fig. 11a). More, contrarily to the previous cases, the shape of the impedance curves remained practically unaltered during the time elapsed testing the sample, highlighting the penetra-
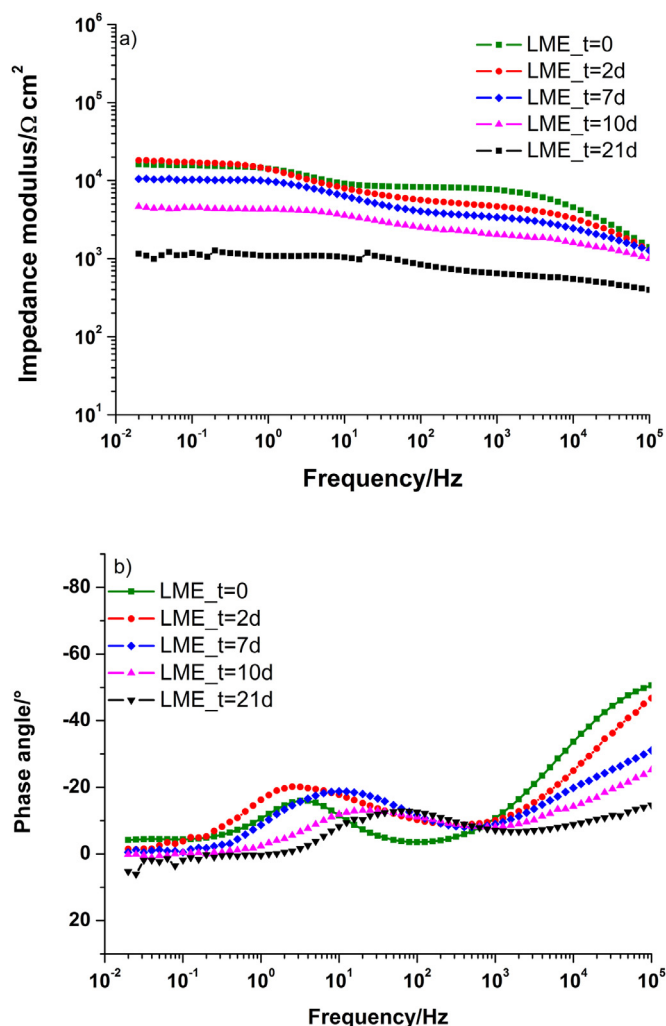
tion of the electrolyte uniformly in the whole organic coating. Looking at the phase angle plot (Fig. 11b) it can be noticed the low value of the phase angle even at the beginning of the test and the resistive sample behavior which extended over a wide range of low frequencies. This behavior could be explained considering the absence of pigments in the coating, that determined the rapid penetration of electrolytes toward the coating/metal interface, so that the corrosion process was started in few hours, determining the delamination of the coating from the metal substrate, which allowed the rapid expansion of the corrosive phenomena.

Fig. 12 discloses the SEM pictures of the LME sample while, in Table 6, its elemental surface composition is reported. As can be seen, in this case, due to the presence of pigments in the epoxy coating (mainly $BaCO_3$ and TiO_2), the coating composition changed very sharply depending on the site of measurement. More, no deposits were found on samples after their ageing in Hank's solution (therefore it was considered useless to show the data) demonstrating that the epoxy resin impeded the formation of layers that, on the con-
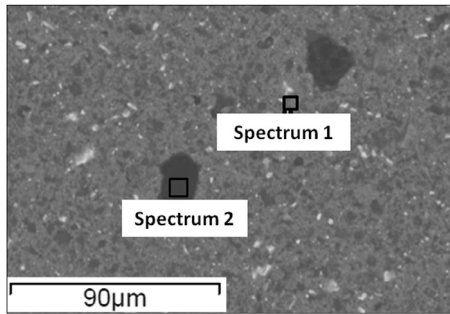
Fig. 12. Scanning electron micrograph of the surface of LME before immersion in Hank's solution.

Table 6
Surface chemical composition of LME sample before immersion in Hank's solution.

Element	Weight%	
	Spectrum 1	Spectrum 2
Carbon	27.06	46.72
Oxygen	25.43	22.96
Magnesium	–	0.24
Aluminium	–	0.75
Sulphur	–	0.20
Titanium	42.92	17.31
Barium	4.59	11.83

Fig. 13. Impedance modulus (a) and phase angle (b) of LMPE sample acquired at 37 °C in Hank's solution.

Fig. 14. Scanning electron micrograph of the surface of LMPE before immersion in Hank's solution.

trary, was formed on the bare metal and PDOPA coated substrate.

In Fig. 13, the Bode modulus and phase angle plots recorded testing the LMPE sample are reported.

The Bode modulus and phase angle plots recorded testing the LMPE sample are reported. As can be seen, the simultaneous action of PDOPA and epoxy resin gave to the sample superior corrosion resistance in comparison to the previously tested samples, underlining the synergistic effect between PDOPA and a polymeric coating. In fact, it was noted that the impedance modulus started from values of $1.7 \cdot 10^5 \Omega$ cm^2, and that after 7 days assumed values of one order of magnitude lower ($1 \cdot 10^4 \Omega$ cm^2), reaching the value comparable to that assumed by the LMP sample.

The slight decrease of impedance modulus at low frequencies (between about 5 and 10^{-2} Hz), as well as the connected increase of phase angle, recorded in performing the EIS test at $t = 0$, which looks like an inductive behavior, has been addressed to the water uptake during the test due to poor barrier coating properties

The phase angle plot (Fig. 13b) clearly showed the triggering of the corrosive phenomenon at the metal/PDOPA interface. In fact, at beginning of the EIS tests, at $t = 0$, a large resistive stretch was shown at low/medium frequencies. After 2 days of exposure to the aggressive solution, a peak appeared, at low frequencies, then the peak moved towards higher frequencies, demonstrating the development of electrochemical phenomena at the interface.

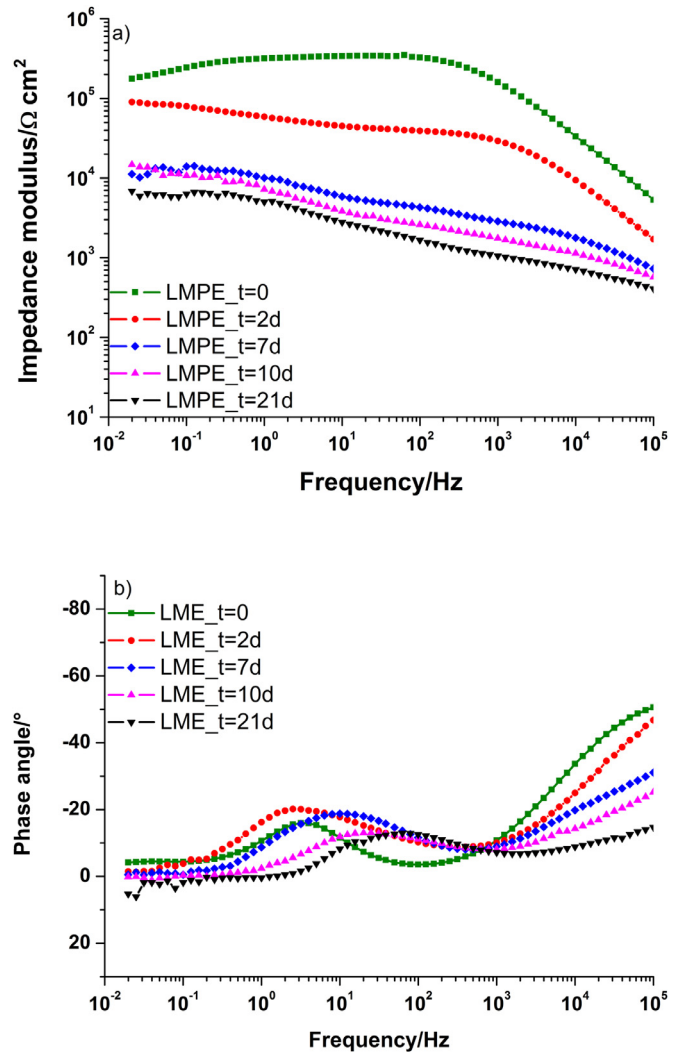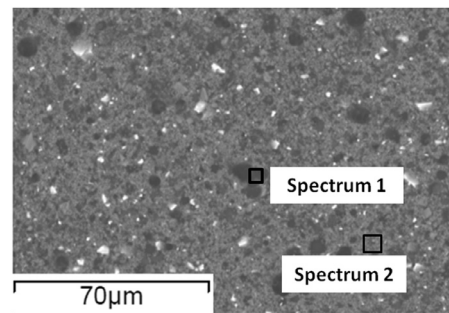Scanning electron micrograph of LMPE sample before exposure to Hank's solution is presented in Fig. 14 while the surface chemical composition is reported in Table 7. The upper layer of the sample was the epoxy resin, so there was the presence of Ti and Ba in the analysed surface, as seen in the LME sample. It was noted a non-uniformity coating composition due to numerous pigments in the epoxy coating.

Table 7
Surface chemical composition of LMPE sample before immersion in Hank's solution.

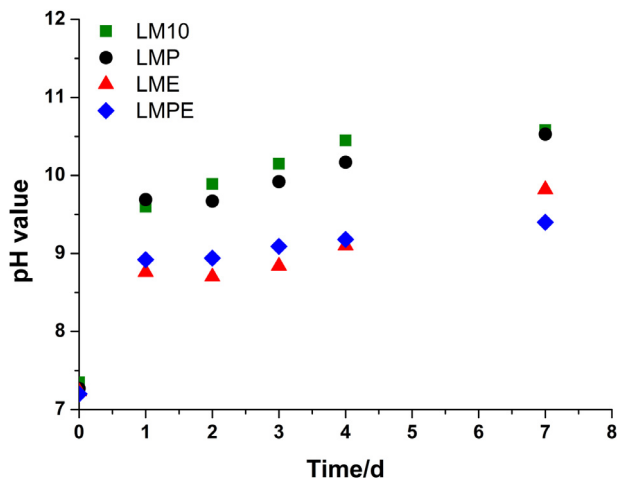| Element	Weight%	
	Spectrum 1	Spectrum 2
Carbon	77.81	31.14
Oxygen	11.83	27.09
Aluminium	–	2.02
Calcium	–	2.88
Titanium	8.12	32.23
Barium	2.24	4.64

Fig. 15. Evolution of pH values of solution during samples immersion period.

After the exposure in Hank's solution, no deposit was found (data not reported) on the surface.

Fig. 15 presents the measured pH values of solution during samples immersion period.

All solutions exhibited a sharp increase of pH in the first day, then, the solutions containing the LM10 or LMP samples reached an pH value of about 10.50 at the end of immersion period, while the pH of the solution containing the samples LME was about 9.80, the solution containing the LMPE sample reached a pH of about 9.40, demonstrating the better protective properties exhibited by the LMPE sample, due to higher barrier effect of this sample. In fact, it had been expected that the solution pH would tend to increase during the corrosion of the Mg alloys [27,30]. When the magnesium is exposed to an aggressive environment, the following reactions take place:

$$Mg \rightarrow Mg^{2+} + 2e^- \tag{1}$$

$$2H_2O + 2e^- \rightarrow H_2 + 2(OH)^- \tag{2}$$

$$Mg^{2+} + 2(OH)^- \rightarrow Mg(OH)_2 \tag{3}$$
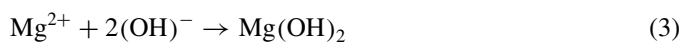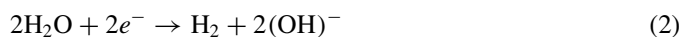
During corrosion, Mg ions dissolve into the solution and pH values increases due to reaction (2). On the other hand, the Mg ions concentration affects the precipitation of calcium

phosphate products, so the increase in the pH value plays a crucial role in the precipitations of these products [31].

4. Conclusions

In this work, the effect of the use of an intermediate layer, consisting of Polydopamine, has been tested, evaluating the degradation behavior of Mg AZ31 samples when immersed in Hank's solution.

Results demonstrated that the PDOPA intermediate coating, deposited between the Mg substrate and the organic coating, decreased the degradation rate of AZ31 magnesium samples during the long-term exposure in the simulated body fluid.

The increase of the pH of the solution was slow down during the immersion period of 21 days, confirming that the sample coated using both PDOPA and epoxy resin, provided better corrosion protection if compared to all other samples. In fact, fair resistance to corrosion was provided by the epoxy coated sample, while the bare and PDOPA coated specimens showed a low resistance comparable to each other and worst of all the samples analysed, as confirmed by EIS results. Due to the approach used in the experimental procedure, these findings cannot be related to the thickness increase of the protective coating.

Conflict of interest

References

[1] H. Shin, S. Jo, A.G. Mikos, Biomaterials 24 (2003) 4353–4364, doi:10.1016/S0142-9612(03)00339-9.
[2] K.-N. Chua, C. Chai, P.-C. Lee, Y.-N. Tang, S. Ramakrishna, K.W. Leong, H.-Q. Mao, Biomaterials 27 (2006) 6043–6051, doi:10.1016/j.biomaterials.2006.06.017.
[3] T. Monetta, A. Acquesta, A. Carangelo, F. Bellucci, Metals 7 (2017) 167–177, doi:10.3390/met7050167.
[4] T. Monetta, A. Acquesta, A. Carangelo, F. Bellucci, Metals 7 (2017) 220–234, doi:10.3390/met7060220.
[5] X. Xiao, Y. Xu, J. Fu, B. Gao, K. Huo, P.K. Chu, Nanosci. Nanotechnol. Lett. 7 (2015) 233–239, doi:10.1166/nnl.2015.1965.
[6] B. Lin, M. Zhong, C. Zheng, L. Cao, D. Wang, L. Wang, J. Liang, B. Cao, Surf. Coat. Technol. 281 (2015) 82–88, doi:10.1016/j.surfcoat.2015.09.033.
[7] B.M. Wilke, L. Zhang, JOM 68 (2016) 1701–1710, doi:10.1007/s11837-016-1869-2.
[8] A. Zomorodian, C. Santos, M. Carmezim, T.M.e Silva, J. Fernandes, M.F. Montemor, Electrochim. Acta 179 (2015) 431–440, doi:10.1016/j.electacta.2015.04.013.
[9] Y. Chen, Y. Song, S. Zhang, J. Li, C. Zhao, X. Zhang, Biomed. Mater. 6 (2011) 025005–025012, doi:10.1088/1748-6041/6/2/025005.
[10] J.H. Waite, Nat. Mater. 7 (2008) 8–9, doi:10.1038/nmat2087.
[11] A. Bourmaud, J. Riviere, A. Le Duigou, G. Raj, C. Baley, Polym. Test. 28 (2009) 668–672, doi:10.1016/j.polymertesting.2009.04.006.
[12] J.H. Waite, Integr. Comp. Biol. 42 (2002) 1172–1180, doi:10.1093/icb/42.6.1172.
[13] X. Liu, J. Cao, H. Li, J. Li, Q. Jin, K. Ren, J. Ji, ACS Nano 7 (2013) 9384–9395, doi:10.1021/nn404117j.

[14] W.-B. Tsai, W.-T. Chen, H.-W. Chien, W.-H. Kuo, M.-J. Wang, J. Bio-mater. Appl. 28 (2014) 837–848, doi:10.1177/0885328213483842.

[15] J. Park, T.F. Brust, H.J. Lee, S.C. Lee, V.J. Watts, Y. Yeo, ACS Nano 8 (2014) 3347–3356, doi:10.1021/nn405809c.

[16] Y. Chen, S. Zhao, M. Chen, W. Zhang, J. Mao, Y. Zhao, M.F. Maitz, N. Huang, G. Wan, Corros. Sci. 96 (2015) 67–73, doi:10.1016/j.corsci.2015.03.020.

[17] L. Huang, J. Yi, Q. Gao, X. Wang, Y. Chen, P. Liu, Surf. Coat. Technol. 258 (2014) 664–671, doi:10.1016/j.surfcoat.2014.08.020.

[18] F. Singer, M. Schlesak, C. Mebert, S. Höhn, S. Virtanen, ACS Appl. Mater. Interfaces 7 (2015) 26758–26766, doi:10.1021/acsami.5b08760.

[19] C. Wang, J. Shen, F. Xie, B. Duan, X. Xie, Corros. Sci. 122 (2017) 32–40, doi:10.1016/j.corsci.2017.03.021.

[20] T. Monetta, A. Acquesta, A. Carangelo, N. Donato, F. Bellucci, J. Magnes. Alloy 5 (2017) 412–422, doi:10.1016/j.jma.2017.09.006.

[21] T. Monetta, A. Acquesta, F. Bellucci, Metall. Ital. 106 (2014) 13–21.

[22] K. Geels, D.B. Fowler, W.-U. Kopp, M. Rückert, Metallographic and Materialographic Specimen Preparation, Light Microscopy, Image Analysis, and Hardness Testing, ASTM international, West Conshohocken, 2007.

[23] C.-C. Ho, S.-J. Ding, J. Biomed. Nanotechnol. 10 (2014) 3063–3084, doi:10.1166/jbn.2014.1888.

[24] Q. Ye, F. Zhou, W. Liu, Chem. Soc. Rev. 40 (2011) 4244–4258, doi:10.1039/C1CS15026J.

[25] A. Acquesta, A. Carangelo, T. Monetta, Metals 8 (2018) 489–499, doi:10.3390/met8070489.

[26] M.R. Zulkifli, M. Zaimi, J.M. Juoi, Z. Mahamud, Mater. Sci. Forum 819 (2015) 303–308, doi:10.4028/www.scientific.net/MSF.819.303.

[27] Y. Xin, C. Liu, X. Zhang, G. Tang, X. Tian, P.K. Chu, J. Mater. Res. 22 (2007) 2004–2011, doi:10.1557/jmr.2007.0233.

[28] T. Monetta, A. Acquesta, A. Carangelo, F. Bellucci, Int. J. Corrosion 2017 (2017) 1–9, doi:10.1155/2017/1541267.

[29] T. Monetta, A. Acquesta, A. Carangelo, F. Bellucci, Metall. Ital. 109 (2017) 91–94.

[30] L. Li, J. Gao, Y. Wang, Surf. Coat. Technol. 185 (2004) 92–98, doi:10.1016/j.surfcoat.2004.01.004.

[31] G. Song, A. Atrens, Adv. Eng. Mater. 5 (2003) 837–858, doi:10.1002/adem.200310405.